A Closer Study of Peak Distortions in Supercritical Fluid Chromatography as Generated by the Injection

Martin Enmark[1], Dennis Åsberg[1], Andrew Shalliker[1,2], Jörgen Samuelsson[1]* and Torgny Fornstedt[1]

[1]Department of Engineering and Chemical Sciences, INTERACT, Karlstad University, SE-651 88 Karlstad, Sweden

[2]Australian Centre for Research on Separation Science, School of Science and Health, University of Western Sydney, Parramatta, NSW, Australia

* Corresponding author

Jörgen Samuelsson PhD

Phone + 46 54 - 700 1620

Mobile + 46 73 932 81 69

Fax +46 54-700 2040

Email: Jorgen.Samuelsson@kau.se

Abstract

In SFC the sample cannot be dissolved in the mobile phase, so it is often dissolved in pure modifier, or another liquid, sometimes resulting in serious distortions of the eluted peak profiles already at moderately high injection volumes. It is suspected the reasons for these effects are solvent strength mismatch and/or viscosity mismatch. This study presents a systematic and fundamental investigation of the origin of these peak deformations due to the injection solvent effects in SFC, using both systematic experiments and numerical modeling. The first set of experiments proved that the injection volume and the elution strength of the sample solution had a major impact of the shapes of the eluted peaks. Secondly, the sample band elution profile was numerically modelled on a theoretical basis assuming both un-retained and retained co-solvent injection plugs, respectively. These calculations quantitatively confirmed our first set of experiments but also pointed out that there is also an additional significant effect. Third, viscous fingering experiments were performed using viscosity contrast conditions imitating those encountered in SFC. These experiments clearly proved that viscous fingering effects play a significant role. A new method for determination of adsorption isotherms of solvents was also developed, called the "Retention Time Peak Method" (RTPM). The RTPM was used for fast estimation of the adsorption isotherms of the modifier and required using only two experiments.

1 Introduction

There is a strong trend towards a revival of Supercritical Fluid Chromatography (SFC) with focus on preparative SFC (Prep-SFC) because of its lower environmental impact and shorter run times as compared to preparative liquid chromatography (Prep-LC). This trend was recently summarized by an extensive review written by the now passed away Georges Guiochon and Abhijit Tarafder [1]; in this article was also listed what was identified to be the major "remaining challenges" for the adaptation of SFC as a reliable chromatographic mode. Today, many Prep-LC

units have been replaced by Prep-SFC units in the pharmaceutical and fine chemical industrial sector, especially for chiral purifications [2]. More recently the revival of SFC has spilled over to the analytical area driven by strong advances in instrumentation [3,4]. The relatively low viscosity of the mobile phase in SFC as compared to LC makes SFC a prime candidate to boost the high throughput trend [5] and leading instrument manufacturers have apparently already have embarked on this road.

Many of the ”remaining challenges” and difficulties with SFC in packed columns resulting in complex behavior [6] are related to the compressibility of the mobile phase in SFC; in a way SFC can be regarded as a “rubber variant of LC” where everything considered as constant in LC is varying in SFC [1]. Altogether, these features of SFC typically result in less reproducibility as compared to LC and poor predictions in scaling up from analytical SFC instruments to preparative SFC instruments. One way of overcoming some of these problems has been to use external devices for measuring the operational conditions in the column [7,8]. Recently, we also employed design of experimental (DoE) approaches to investigate which operational parameters are most important to control for reliable transfer of methods between different system and scaling up for some uncharged compounds [9,10].

In SFC the sample cannot readily be dissolved in the mobile phase, so it is often dissolved in a liquid, or the modifier itself. This can result in solvent strength and viscosity sample solvent-mobile phase mismatch. The mismatch, already at low to moderate high sample volumes, will often result in serious distortions of the eluted peak profiles. These combined effects are often simply denoted as “plug effects” [11,12]. It is well-known from LC that injecting the solute in an injection solvent with stronger elution strength as compared to the bulk mobile phase leads to severe and complex band distortions especially at large injection volumes/loads [13–15]. It can be suspected that the underlying reason for these “plug effects” are even more complex in SFC and might also be due to viscous fingering effects (see below). However, except for an experimental study [12], experimental and simulated by Yun et al [11], or purely theoretical ones [16] there are few studies in SFC aiming at combining experimental evidence and

quantifying these phenomena using a modeling approach. In this study we are going to investigate the plug effect utilizing a combined experimental and modelling approach.

There are two main injection principles in SFC [17,18] : (i) the mixed-stream injection mode and (ii) the modifier-stream injection mode, respectively (see Figure 1). In the first injection mode, the injection is conducted prior to the column after the CO_2 stream and modifier have been mixed (*cf*. Figure 1a). The second mode is only used in Prep-SFC and requires that the injection is made in the modifier-stream, which is then mixed with the CO_2 stream (*cf*. Figure 1b). Each injection technique has its potential advantages and disadvantages and these were recently evaluated in preparative SFC by Miller and Sebastian [18]. They found that modifier-stream injection was advantageous for many cases, especially for high-volume injections and for solutes having a low retention factor, which were markedly disturbed when performing mixed-stream injections. In a recent publication these problems were realized experimentally and the authors suggested viscous fingering was a principle factor influencing the observed peak distortions, when utilizing the mixed-stream injection mode [11].

When a viscosity mismatch between two fluids is apparent, and one fluid pushes the other, a phenomenon known as viscous fingering (VF) can occur. More particular, in SFC a high viscosity fluid (the 'plug') pushes a lower viscosity fluid (the eluent) and the leading interface sharpens. At the same time the trailing interface of the sample band (plug) is penetrated by the lower viscosity mobile phase in a complex manner that resembles fingers [19–22]. In SFC the mobile phase has a lower viscosity than the injection plug, and this viscosity contrast is quite large. However, still no one has investigated and experimentally proved the effects also occur in SFC. Physical evidence of the VF phenomena in liquid chromatography has been obtained by several research groups [23,24]. Shalliker et al [25,26] used glass columns and a mobile phase which had the same refractive index as the C18 silica; hence, the otherwise opaque column bed became perfectly transparent. The viscosity between the injection plug and the mobile phase could be adjusted and the VF effect visualized either with the aid of colored samples or by injection of a solvent with a different refractive index to the mobile phase.

The aim of this investigation is to gain a deeper understanding of the major underlying reasons for the peak distortions taking place already at low to moderate high sample volumes in SFC. Especially, we aim at investigating the relative impact of the solvent strength and the viscous contrast mismatches, respectively. To investigate this, a three step approach was applied. First, we investigated and compared experimentally modifier- and mixed-stream injections as well as the effect of the sample's elution strength. Secondly, the sample elution band from mixed stream injections was numerically modelled assuming effects of both un-retained and retained co-solvent, respectively. Finally visualization experiments were conducted using liquid conditions with a viscous contrast between the eluent and sample solution similar to what would be observed in SFC conditions. For estimating the modifier adsorption isotherm without using large injections a new adsorption isotherm acquisition method was developed, the "Retention Time Peak Method" (RTPM).

2 Theory

2.1 Calculating the methanol volume fraction

For simulation of chromatographic experiments, the volumetric fraction of methanol in the eluent was used. However, the instrumentally set conditions need to be verified as they cannot be assumed to be the same as the actual conditions. To calculate this we need to estimate the molar volume of carbon dioxide and methanol. The molar volume of the fluid (*V*) was calculated according to Kato et al. [27]:

$$V = \frac{M}{\rho} \quad , \qquad (1)$$
$$M = x_{CO_2} M_{CO_2} + x_{MeOH} M_{MeOH}$$

where M is the molecular weight of the fluid, ρ is the mass density of the fluid and x is the mole fraction. To estimate the volumetric fraction, the partial molar volume (V_i) needs to be calculated. It could be calculated according to [27]:

$$V_{CO_2} = V + x_{MeOH} \frac{\partial V}{\partial x_{CO_2}}$$
$$V_{MeOH} = V - x_{CO_2} \frac{\partial V}{\partial x_{CO_2}} \quad (2)$$

For a more in depth discussion about Eq. 2(a, b) see eqns. 4 and 5 in Kato et al.[27].

From the calculated molar volume and measured mass flows $\dot{m}$ of carbon dioxide and MeOH it is straight forward to calculate the volumetric fraction of MeOH:

$$v\%MeOH = \frac{\frac{\dot{m}_{MeOH}}{M_{MeOH}} V_{MeOH}}{\frac{\dot{m}_{MeOH}}{M_{MeOH}} V_{MeOH} + \frac{\dot{m}_{CO_2}}{M_{CO_2}} V_{CO_2}} \cdot 100 \quad (3)$$

The density of the fluid were estimated using the Kunz and Wagner [28] equation of state as implemented by the National Institute of Standards and Technologies in REFRPOP v 9.1. The necessary inputs are the mass fractions of carbon dioxide and methanol, pressure and temperature. The molar fractions were estimated using the measured methanol and total mass flow. $\partial V/\partial x$ were numerically estimated by integrating REFPROP database in CoolProp [29] using a Python 3.x wrapper.

2.2 Chromatographic modeling

In this study the elution profiles were calculated using the equilibrium-dispersive (ED) model of chromatography [30]. In this model the Langmuir model [31] was used to describe the distribution of solutes between the stationary and mobile phases. The Langmuir model could be expressed as:

$$q = q_s \frac{KC}{1 + KC}, \quad (4)$$

where q_s is the monolayer saturation capacity and K is the association equilibrium constant. In chromatography, a compound adsorption described using the Langmuir model will result in right angled-triangular shaped elution zones.

2.3 Simple new method for adsorption isotherm estimation

In this study the adsorption isotherm of methanol was determined using the following simple approach:

1. The initial slope of the adsorption isotherm was estimated from the retention time of a perturbation peak obtained when using an eluent of pure carbon dioxide.
2. The association equilibrium constant was estimated from the retention time of a perturbation peak using an eluent with methanol.

Using this new method it is assumed that the adsorption isotherm of methanol is described using a Langmuir model in this study. From now this method is going to be called "Retention Time Peak method" (RTPM). This method is not limited to just using the Langmuir adsorption isotherm or for determination of co-solvent. Below is a general presentation of the method.

If a small excess of a compound is injected into a column already equilibrated with a mobile phase containing the same compound a peak will be detected [30,32,33]. This peak is generally called the perturbation peak, the retention time (t_R) of which is dependent on the concentration (C_i) of the concentration plateau and could be calculated as:

$$t_R(C_i) = t_0\left(1 + F\left.\frac{dq}{dC}\right|_{C=C_i}\right), \quad (5)$$

where t_0 , F and dq/dC are the holdup time, the phase ratio (ratio between the stationary and mobile phases) and the slope of the adsorption isotherm, respectively.

The slope of the adsorption isotherm is estimated experimentally without any compound in the eluent, in other words $C_i = 0$. In this case the initial slope of the adsorption isotherm could be estimated as:

179 $$\left.\frac{dq}{dC}\right|_{C=0} = \frac{t_R(0) - t_0}{Ft_0}. \quad (6)$$

180 Now we need to assume an adsorption isotherm model. In this study we use the Langmuir
181 model, but other models could also be used. For the Langmuir adsorption isotherm, Eq. (4), the
182 initial slope of the adsorption isotherm is equal to $q_s.K$. To estimate the association equilibrium
183 constant in the Langmuir model the retention of a perturbation peak is determined using a
184 column equilibrated with a mobile phase containing the same compound with a concentration
185 of C_i:

186 $$b = \frac{\sqrt{q_s K} - \beta}{C_i \beta}, \quad \beta = \frac{t_R(C_i) - t_0}{Ft_0} \quad (7)$$

187 The RTPM for determination of adsorption isotherms is based on the same theory as the
188 perturbation peak (PP) method [30,33]. The advantage of the RTPM over the PP method is that
189 fewer experiments are required to determine the adsorption isotherm for the simple
190 adsorption isotherm models. The major drawback is that the adsorption model is needed to be
191 assumed in advance. As a consequence no raw adsorption data is generated. This means that
192 no further insight about the adsorption process, from tools such as Scatchard plots and
193 adsorption energy distribution calculations [34,35] can be obtained. Another drawback is that
194 the experiments need to have higher accuracy compared to the PP method, because no
195 redundant experimental data are used. Another similar and fast method to estimate the
196 adsorption isotherm is the Retention Time Method (RTM) [30]. In the RTM method the initial
197 slope is estimated from an analytical injection and the association equilibrium constant is
198 estimated from the sharp front of an overloaded elution profile [30]. To get overloaded elution
199 profiles for the RTM substantial injection volumes are needed, that could result in peak
200 distortion and therefore unreliable adsorption parameters. This is no problem for RTPM,
201 because the adsorption data is determined from the retention time of analytical small volume
202 injections. The RTPM method could readily be expanded to other adsorption models using
203 similar approaches as for RTM [7].

3 Experimental

3.1 Chemicals

HPLC grade methanol, 2-propanol and heptane (Fischer Scientific, Loughborough, UK), CO_2 (> 99.99%, AGA Gas AB, Sweden), toluene (Analar normapur, VWR Chemicals) dichloromethane (Analar normapur, VWR Chemicals), cyclohexanol (99%, Sigma-Aldrich) and ethanol (99.7%, VWR Chemicals) were used as solvents and mobile phase. As solutes antipyrine (Ph. Eur., Fluka Analytical) and salicylanilide (98%, Aldrich Chemicals) were used. In the viscosity experiments Oil-Red 'O' dye (Sigma-Aldrich) was used to visualize the injection plug. The columns used in this study were packed with Kromasil Diol (5 µm nominal particle size, 60 Å pore size Akzo Nobel, Bohus, Sweden) in 4.6×150 mm tubes. One column was used in SFC experiments and the other in LC experiments. In the viscosity experiments an HR glass column (5 mm, I.D.) Pharmacia (Uppsala, Sweden) was packed with Kromasil-100-5-C18 (100 Å pore and 5 µm particle size) (Akzo Nobel, Bohus, Sweden) using axial compression.

3.2 Instrumentation

The SFC experiments were performed using two Waters UPC^2 systems (Waters Corporation, Milford, MA, USA) each equipped with a 100 µL loop. The first UPC^2 was equipped with a PDA detector and the second was interfaced to a Waters SQD single quadrupole (Waters Corporation, Milford, MA, USA) interfaced using APCI. Effluent from UPC^2 was diluted with 0.2 mL/min methanol, probe temperature was 350 °C and cone voltage 30 V. Manually tuned selective ion monitoring at 37 m/z.

To determine accurate volumetric flow and volume fractions of methanol, the first UPC^2 was interfaced to additional pressure transmitters (model EJX530A (Yokogawa Electric Corporation, Tokyo, Japan) and a Coriolis based mass flow meter (Bronkhorst mini CORI-FLOW model M12 (Bronkhorst High-Tech B.V., Ruurlo, Netherlands). For more information about the measuring procedure, the reader is referred to the recent publication by Enmark et al [8].

The HPLC experiments were performed on an Agilent 1200 system (Agilent Technologies, Palo Alto, CA, USA) equipped with a binary pump, an auto sampler, a diode-array UV-detector and a thermostated still air column oven.

For the viscosity experiments a Jasco PU 1580 HPLC pump (JASCO, Japan) was used for the delivery of all mobile phases. A Midas auto injector from Spark Holland (AJ Emmen, The Netherlands) was used for sample injection. Detection was achieved photographically using a Nikon D5100 SLR camera (Nikon Corporation, Japan) fitted with a variable focal length 18 to 300 mm lens (Nikon Corporation, Japan) fixed at 300 mm for image acquisition. The f-stop was set at 10, and the camera was operated in video record mode. Still photographs were taken as 'snap-shots' from these videos using Adobe Photoshop CS6 and processed later using Inkscape 0.91 (Open Source software). In order to minimize the cylindrical lens effect of the tubular column, the column was housed in a standard 30 × 40 × 30 cm tank, which was illuminated using an 8 Watt white fluorescent light tube (Diversa, Poland) located directly behind the column.

3.3 Procedure

To investigate the effect of injection volume and injection solvent on peak distortion in mixed-stream injection mode, experiments were performed using the method set conditions of 10/90 v% methanol/CO_2, 1 mL/min, back-pressure of 150 bar and a temperature of 30°C. Volumes from 2 to 75 µL were injected. Concentrations of 0.5 to 300 g/L antipyrine and 0.5 to 60 g/L salicylanilide diluted in MeOH were separately injected for each volume in at least duplicate. Separate solutions of ca 0.2 g/L antipyrine and 0.2 g/L salicylanilide diluted in methanol, ethanol and toluene were also prepared and injected between 2 to 75 µL. All low volume and low concentration injections were monitored at 220 nm while high concentration injection of antipyrine and salicylanilide were recorded at 310 and 350 nm respectively.

Injections of pure methanol between 2 to 75 µL were also performed and recorded at 202 nm. These injections were complemented by mass spectrometric detections. Injections of 2 to 60 µL

pure MeOH-d4 was made in duplicate. The abundance of the 37 m/z ion was recorded in selective ion monitoring mode.

To investigate the effect of injection volume on peak distortion in modifier-stream injection mode, the UPC^2 system using a PDA detector was reconfigured for modifier-stream injections by diverting the modifier flow to the injection valve and then mixing this flow with the carbon-dioxide stream in a low volume tee just prior to the column. Volumes of 5, 30 and 75 µL of 0.25 to 300 g/L antipyrine and 0.5 to to 60 g/L salicylanilide were diluted in MeOH and separately injected. The running conditions were identical to the mixed-stream injection mode.

The dependence of the retention factor and adsorption isotherm of antipyrine and salicylanilide on the v% methanol was investigated on 5, 10, 15, 20, 25, 30, 40, 60, 80 and 100 v% methanol. All other running conditions were identical to the other experiments. On each methanol level, 2, 5 and 10 µL of 0.25 to 300 g/L antipyrine and 0.4 to 60 g/L salicylanilide were injected. Wavelengths of 220, 310 and 355 nm were used to record chromatograms.

The column void volume was estimated from the retention time of N_2O dissolved in methanol at 5 v%, which has previously been shown to be a stable estimate of column void volume. The system void volumes were estimated by from the breakthrough times of dilute injections of antipyrine when replacing the column with a “zero” volume union. This was done in both mixed-stream and modifier-stream injection mode.

The HPLC experiments were done with 15/85, v%, ethanol/heptane as mobile phase, the column was operated at 30°C, the flow rate was set to 2.0 mL/min and detection was done at 220 nm. Duplicate injections were done with solutions of ca 0.2 g/L of antipyrine or salicylanilide. The solutes were dissolved in ethanol, propanol and mobile phase with injection volumes of 2 µL and 75 µL.

In the viscosity experiments a sample of Oil Red O dye was dissolved in 45:55 DCM: Toluene (viscosity of 0.38 cP), which was used as a visualization agent. Two mobile phases were used one without a viscosity contrast (45:55 DCM: Toluene) and the second with a viscosity contrast of approximately 3.8 times (19:24:57 DCM: Tolene: cyclohexanol (viscosity of 1.44 cP)). The viscosity values are derived from previous work by Catchpoole et al. [21]. In these experiments the mobile phase flow rates were set at 0.5 mL/min. and injection volumes were 5 μL.

3.4 Calculations

The elution profiles were calculated using the equilibrium-dispersive (ED) model of chromatography [30] solved by using the orthogonal collocation on finite elements (OCFE) method [36,37]. To discretize the spatial derivatives of the ED model the Adams-Moulton method implemented in the VODE procedure [38] was used to solve the system of ordinary differential equations. In these calculations the efficiency was assumed to be 5000 and the numbers of subdomains used in the calculation were set to 500.

The adsorption isotherms of antipyrine were determined using the elution by characteristic method in slope mode [39]. Using the ECP method it is necessary to have a calibration curve to convert detector response (R) to concentration (C), this was done by fitting the detector response for three different column loads for each condition to Eq. (8) so that the injected mass is equal to eluted mass.

$$C = k_1 \log\left(\frac{k_2 - R}{k_2}\right) + k_3 R \qquad (8)$$

where k_1, k_2 and k_3 are constants used in the calibration curve.

The adsorption isotherm dependency on methanol content was estimated by fitting determined adsorption isotherm for antipyrine at set conditions of 10, 15, 20, 30, 40, 60, 80 and 100 % MeOH to a cubic polynomial.

316

317 All calculations except for OCFE were conducted using open source software Python 3.4.2,
318 Numpy 1.9.1, Scipy 0.15.1 and Matplotlib 1.4.3.
319

320 ## *4 Results and discussion*

321 In this study we are investigating the major underlying reasons for elution peak distortion
322 caused by the solvent plug that occurs as a sample is introduced in SFC using a different sample
323 solvent compared to the eluent. First, in Section 4.1, observations are made from experiments
324 using the two dominating injection modes: injections in the modifier and in the mixed-stream,
325 respectively. Here, it will be discussed how these experiments can be attributed to the sample
326 solvent effects and the adsorption behavior will be classified in a qualitative way. Secondly, the
327 elution strength of the injection solvent is investigated (Section 4.2). In Section 4.3 solute
328 elution profiles were calculated by using a plug model assuming that the injection creates an
329 un-retained sample solvent plug that affects retention of the solute. Finally in section 4.4,
330 sample zone broadening will be investigated. In this section, first solvent adsorption is studied
331 by both experiments and modeling. Secondly, band broadening due to viscosity contrast
332 between sample solvent and mobile phase is experimentally visualized and discussed.

333 ### *4.1 Injection mode and adsorption observations*

334 The most common injection mode in SFC, which is utilized by all major commercial SFC
335 instruments, is the mixed-stream injection mode (*cf*. Fig. 1a). Alternatively, the modifier-stream
336 injection mode allows (*cf.* Fig 1b) the sample to be introduced into the modifier-stream prior to
337 the mixing point between carbon dioxide and modifier. Usually in mixed-stream injection it is
338 most likely that the composition of the injection solvent will be different from the eluent. For
339 modifier-stream injection, the injection solvent can be chosen to be identical to the modifier
340 blended with carbon dioxide. To study the peak deformation obtained using the two injection
341 modes, two small organic molecules, antipyrine and salicylanilide were studied. In Fig. 2(a-b) 5,
342 30 and 75 µL of 0.25 g/L and 100 g/L antipyrine injections are presented for mixed and
343 modifier-stream injection. In Fig. 2(c-d) 5, 30 and 75 µL of 0.5 g/L and 20 g/L salicylanilide are

presented. From visual inspection the resulting profiles from low-concentration injections of antipyrine and salicylanilide in Fig. 2(a, c), it is apparent that high volume injections in the mixed-stream injection mode gives markedly deteriorated elution profiles, while the equivalent injections in the modifier-stream injection mode does not. The center of mass of the elution profile obtained in mixed-stream injection mode is shifted to shorter retention times, while it remains approximately constant for the modifier-stream injections. Only when injecting 5 µL is the elution profile obtained in the two modes similar, regardless of injected concentration. The elution profiles obtained from the high concentrated samples gives insight into the adsorption behavior of the solutes. The left angled-triangular elution profile for antipyrine, see Fig 2. (b), indicates that antipyrine follows "Langmuirian" adsorption (Eq 4). For salicylanilide the overloaded elution profiles are right angled-triangular shaped, indicating that salicylanilide follows "anti-Langmuirian" adsorption, see Fig. 2(d). However, further experiments would be required to verify the origin of this observation.

The trend of shifting the center of mass of the elution profiles to shorter time when injecting the sample in higher elution strength diluent has previously been reported in SFC [12] where the conclusion was to (1) inject as small volumes as possible and (2) use a less polar injection solvent.

4.2 Changing elution strength of sample solvent

Common practice in SFC is to dissolve the sample in the organic modifier, e.g. methanol, which has a much stronger "solvent strength" compared to CO_2, while in Normal Phase Liquid Chromatography (NPLC) the sample is often dissolved in the mobile phase. To investigate the effect of the solvent strength on the elution peak shape three different solvents were used to dissolve the sample and the effects in NPLC and in SFC are compared.

In SFC the mobile phase was 7.2 v% MeOH. The effect of the injection solvent was investigated by using toluene, methanol and ethanol as sample solvents. Toluene was selected because it is more nonpolar solvent compared to the alcohols and therefore closer in elution strength of the eluent. In NPLC, the same stationary phase was used, but the eluent was 15/85, v/v,

ethanol/heptane and as injection sample solvents ethanol, 2-propanol and 15/85, v/v, ethanol/heptane were used. Because methanol is immiscible in heptane, 2-propanol was used instead. Injections were done at two different injection volumes; 2 and 75 µL with the solutes dissolved as described above. The profiles obtained from 2 µL injections overlapped perfectly for all sample solvents in both SFC and HPLC (not shown). This indicates that there are no injection plug-phenomena when the injection volume is small enough relative to the actual column volume, which agrees very well with previous reversed phase liquid chromatographic observations [14,15].

One way of comparing the solvent strength is to use the eluent strength (ε_0) on SiO_2, defined by Snyder as the adsorption energy of the solvent adsorbing on the stationary phase per unit area [40]. High adsorption energy means high eluent strength in NPLC mode. Since the eluent strength was determined for silica adsorbents and here a Diol stationary phase was employed, the values of the eluent strength should be treated as approximate and only the relative order of the solvents are used in this discussion. The solvent strengths for sample solvents according to $\varepsilon_0(SiO_2)$ and dielectric constant is presented in Table 1, data from [41].

In NPLC when 75 µL was injected, Fig. 3b and 3d, the degree of peak distortion was largest for the sample dissolved in ethanol, which has the largest eluent strength contrast between the eluent and the sample solution, followed by isopropanol (second largest) and lastly mobile phase. The same trend was evident in SFC - Fig 3a and 3c, where methanol has the largest eluent strength contrast between the sample and the eluent and subsequently the largest peak distortions were apparent followed by ethanol and toluene with minor peak distortion. Finally, one could observe that for salicylanilide in NPLC, Fig 3d, which had a smaller retention factor compared to antipyrine, Fig. 3b, the peak distortions were more pronounced, as expected for solute that elutes closer to the void.

The deformations of the peaks seen in NPLC and in SFC are qualitatively the same. This indicates that the plug-phenomena are similar in NPLC and SFC. Dissolving the sample in a

solvent with similar elution strength as the mobile phase seems to minimize the peak distortion in SFC, which agrees with previous results [12].

4.3 Prediction of elution profiles

So far it has experimentally been shown that the injection solvent will affect the elution profile. Now we will investigate if it is possible to quantitatively describe the distortion of the elution profile when injecting different 2-75 µL of 0.25 g/L of antipyrine dissolved in methanol. Salicylanilide was not chosen due to its apparently more complex adsorption mechanism. To qualitatively describe the propagation of the solute through the column when the solutes in the sample solution have different adsorption properties than in the eluent the following assumptions were made,

1. The injection creates an un-retained solvent plug that travels along the column. The sample zone broadening along the column is only due to dispersion in the separation system. In other words methanol is simulated as a compound with no retention.
2. The solute retention is modifier dependent and this dependency is only manifested in the adsorption isotherm.

The assumptions above gives a simple model that is similar to the "plug model", which was previously used to describe how pH-mismatch between sample solution and eluent affects the elution profile [13]. In the pH study the chromatography was modeled using the ideal model (efficiency is infinite) solved using characteristic lines approach. Yun et al have also analyzed the plug phenomena using a similar approach [11]. In Yun et al the plug is modeled using the ED model and linear adsorption isotherm were used to describe the retention of the solutes. In this study the adsorption of antipyrine is assumed to be described using the Langmuir model. As in the study by Yun et al the MeOH fraction was also simulated. However, instead of using mass fractions as in the case by Yun et al, we instead used volume fractions; see Section 2.1, in order to get better correlation with concentrations used in the Langmuir model, see eq. (4).

The adsorption isotherm for antipyrine was determined using the slope elution by characteristic point method [39] at different fractions of modifier. As already has been shown in Fig. 2b,

antipyrine's elution profiles are right angled-triangular wherefore the Langmuir model was chosen. The adsorption isotherm was determined using 5 µL injection of 300 g/L antipyrine on eluents with 7.2, 18.0, 29.6, 40.5, 60.2, 79.7 and 100 v% MeOH (set conditions of 10, 20, 30, 40, 60, 80 and 100). Injections of 5 µL were used because the analytical elution profiles from mixed and also in modifier injection mode were coincident, see Fig. 2. The resulting adsorption isotherm parameters are presented as symbols in Fig. 4. To be able to use this data in the ED model the determined adsorption isotherm parameters were fitted to a cubic function, see grey line in Fig. 4.

The experimental elution profiles for the injection of 2, 5, 10, 20, 30, 60 and 75 µL injections of 0.25 g /L of antipyrine in MeOH and eluent of 7.2 v% MeOH, are presented as black line in Fig. 5a. In Fig. 5b, the corresponding calculated elution profiles are presented. Comparing the experimental and calculated elution profiles one could see that the elution profiles are very similar. The main differences are noted at high injection volumes (60 and 75 µL) where the simulated profiles were less distorted. Also note that the experimental elution profiles were slightly broader than the simulated profiles. Yun et al studied 5, 50, 1000 and 2000 µL injections and in contrast to our study they found that generally the simulated profiles were broader compared to the experimental profiles [11].

In Fig. 5c, simulated elution profiles assuming expanding injection plug is shown, this will be discussed later in Section 4.4.1.

4.4 Sample zone broadening

The above results clearly indicate that the solvent strength is a main contributing factor responsible for peak distortion. However, as noted, the simulated elution peaks were not as broad or distorted as the experimental peaks, indicating that other factors may also be responsible for peak distortion. Below two other contributing factors are discussed, first solvent adsorption to the stationary phase thereafter viscosity mismatch between sample and solvent, and eluent.

Another factor that could cause band broadening is that the injection of pure methanol may cause a pH plug with lower pH due to that alkyl-carbonic acid is formed in MeOH/CO_2 environment [48]. However, this potential pH plug will only very weakly affect the solutes ionization under investigation and have some slight effect on the polarity of the stationary phase. Therefore it is believed that the potential pH plug will have a very minor effect on the studied experimental systems.

4.4.1 Solvent adsorption

Referring back to the simple plug model described above (Section 4.3) it was assumed that the injection creates an un-retained solvent plug that travels along the column. However, several studies have shown that MeOH adsorbs to the stationary phase [42,43]. If MeOH adsorbs to the stationary phase, the injection plug will be diluted and unsymmetrically broadened. To investigate MeOH adsorption to the stationary phase; 2, 30 and 60 µL injection of MeOH were injected on an eluent containing 7.2 v% MeOH and detected using a UV detector at 202 nm, see Fig 6a. As can be seen the elution profiles presented are right angled-triangular, which indicates that MeOH actually adsorbs to the stationary phase. The shape also indicates that the adsorption of methanol could be described using a type I adsorption model [44]. One drawback with these experiments is that the signals are deformed and very noisy. One must stress that the signal recorded using a UV detector are actually not originating from the injected molecules, but instead from displaced molecules from the eluent that are already adsorbed to the column [42,45]. To detect the injected molecules they must be labeled, using for example, deuterium [46] and then detect them using a selective detector that could distinguish between labeled an unlabeled molecules. Often the displaced elution zone is called the “perturbation peak” and the elution zone containing the injected molecules the “tracer peak”. To get a better insight the experiments were redone, but now with deuterium labeled MeOH (CD_3OD) instead of regular MeOH see Fig 6b. The signal was detected using SIM mode (37 m/z). The elution profiles in this case were left angled-triangular shapes and eluted after the perturbation peak. This observation is expected for tracer pulses when the adsorption of MeOH is described using a type I adsorption isotherm [47]. UV and MS traces of the methanol injection clearly indicate that MeOH adsorbs to the stationary phase and subsequently this will result in plug broadening.

To model the MeOH injection, the adsorption is assumed to be described using a Langmuir adsorption isotherm and the adsorption isotherm was estimated using the RTPM, described in Section 2.3. The initial slope of the adsorption isotherm was estimated from the retention time (35 min.) of methanol using pure carbon dioxide and the association equilibrium constant was estimated from the retention of the perturbation peak of methanol using a 2 µL injection, using an eluent with 7.2 v% MeOH.

With this data the elution profiles for injections of 2, 5, 10, 20, 30, 60 and 70 µL of 0.25 g/L of AP in MeOH and eluent of 7.2 v% MeOH were again simulated, but now methanol was assumed to be retained, see Fig. 5c. Comparing the simulated elution profiles with and without methanol adsorption we could see only minor differences. The main observed difference is that the predicted elution profiles are slightly broader from the model with methanol adsorption, see Fig. 5c.

In Fig. 6c, the predicted methanol elution profiles are presented. Comparing experimental methanol elution profiles in Fig. 6a, we see that the predicted methanol elution profiles were not as broad as the experimental ones. One explanation to this observation could be the viscosity mismatch between the sample solution and the eluent.

4.4.2 Viscous fingering effects

The viscosity of a CO_2 mobile phase containing 7.2 v% MeOH at 150 bar and 30 °C is around 0.16 cP [49]. The viscosity of methanol is 0.59 cP. Thus the viscosity contrast between eluent and injection solvent is in the order of at least 3.7 times. To experimentally visualize viscosity effects of this magnitude we performed experiments in glass columns using a matched refractive index between the stationary phase and the mobile phase. Under these conditions the opaque stationary phase is transparent. In this study 5 mm I.D. columns were packed with a 5µm C18 silica phase and equilibrated with 45/55 v% dichloromethane/toluene, which has a viscosity of 0.38 cP. This mobile phase has the exact same refractive index as the C18 silica. Fortuitously, cyclohexanol has a very high viscosity, and the same refractive index as the

stationary phase. Hence the viscosity of the mobile phase can be easily adjusted simply by adding cyclohexanol to the dichloromethane/toluene mixture. The injection was visualized by adding an un-retained colored dye to the sample [19–22,50].

Two experiments were conducted; the first with no viscosity contrast between the eluent and the sample solution, see Fig. 7a. The second experiment was performed such that there was a viscosity contrast between the injection solvent and the mobile phase of approximately 3.8 times, see Fig. 7b. The sample zone in the column without viscosity contrast, Fig. 7a, is more or less bullet-shaped whereas this is not the case when there was a viscosity contrast (*cf.* Fig. 7b). From inspection of these images we can clearly see that the sample zone was distorted and severely tailing and this would drastically broaden the elution zone of the injection solvent. We strongly believe that the observed extra band broadening of the methanol plug in Fig. 6 is primarily a consequence of the viscosity contrast between the eluent and the sample solution. This will result in a broader sample zone that propagates through the column and in that way can interact with the solute and result in broader solute elution profiles as observed in Fig. 5. Such broadening effects will occur even for retained solutes since the band distortion associated with the viscosity contrast effect takes place the very instant that the solute injection plug enters the column.

5 Conclusions

The dominating injection technique in SFC, mixed-stream injection, was investigated through experimentally based modelling and was compared with modifier-stream injection. Modifier-stream injections allow for experiments without injection plug effects by injection in the modifier stream prior to the mixing chamber. It was observed that mixed-stream injections gave rise to significant peak distortion even at moderately large injection volumes, which were not present in the modifier-stream injection mode. The peak distortions observed in this study will have the most pronounced effect at preparative-scale injection volumes. In the analytical case, generally smaller volumes are injected so little if any distortion would be expected. Previous studies have shown strong indications that these distortions (plug effects) are a

combined solvent and viscous fingering effect. Therefore, our focus was to distinguish between the two effects qualitatively and as quantitatively as possible.

First, the effect of the solvent strength and viscosity of the diluent on the peak shape was studied in both SFC and NPLC. It was evident that the trends were similar for SFC and NPLC; the solvent strength was much more important than the viscosity and injection in a diluent with similar solvent strength as the mobile phase resulted in less peak distortions. The center of mass of the elution profiles in both NPLC and SFC were shifted to shorter retention times when injecting the sample in diluent of higher elution strength.

Secondly, two sets of calculations of the elution bands were performed where the solvent was assumed to be un-retained and retained, respectively. For un-retained solvent the calculations confirmed quantitatively the empirical conclusions from above; that the solvent strength contrasts are the main reason for the distortions. Still the experimental elution profiles were broader than the predicted ones, even when theoretically taking into consideration solvent adsorption onto the stationary phase, which resulted in broader elution profiles, but not as broad as the experimental ones. This also confirms that there is an additional source for broadening and distortion of the elution bands especially at large injection volumes.

The additional source of this band broadening could be due to viscous fingering and this hypothesis was investigated through HPLC experiments imitating the SFC conditions. It was shown that viscous fingering was indeed present in these experimental conditions, which employed 5 mm I.D. columns, similar to the 4.6 mm I.D. columns used in HPLC and SFC experiments. The sample zone was distorted at the leading edge and severely tailing, both factors will drastically broaden the elution zone of the injection solvent. We believe that the observed extra band broadening of the solvent plug is a consequence of the viscosity contrast between the eluent and the sample solution.

We conclude that the contrast between the elution strength of the sample solvent and the eluent is the main reason for the peak distortions. The next most important factor is viscous fingering effects that can cause some additional band broadening. The solvent adsorption effect had only minor effect on the band broadening. A general conclusion regarding the maximum possible injection volume without causing peak distortion will also be a function of the retention factor of the solute. Based on the experimental findings presented here, no peak distortions occur at 5 µL injections, but Fairchild recently showed severe distortions already at 2 µL injections [12]. A more comprehensive study entailing several solutes with different retention factors as well as different sample solvents would likely allow for more exact guidelines. Importantly we have shown that separating the various factors that lead to band broadening is a complicated task and improving separation performance may require a multifaceted approach to optimize the sample injection protocol.

Acknowledgement

This work was supported by the Swedish Research Council (VR) in the project "Fundamental studies on molecular interactions aimed at preparative separations and biospecific measurements" (grant number 621-2012-3978) and by the Swedish Knowledge Foundation for the International visiting Professor Andrew Shalliker (grant number 20140028). The authors wish to thank Andrew Aubin at Waters Coporation for discussions on how to modify the UPC^2 system for modifier-stream injections.

References

[1] G. Guiochon, A. Tarafder, Fundamental challenges and opportunities for preparative supercritical fluid chromatography, J. Chromatogr. A. 1218 (2011) 1037–1114.

[2] M.A. Lindskog, H. Nelander, A.C. Jonson, T. Halvarsson, Delivering the promise of SFC: A case study, Drug Discovery Today. 19 (2014) 1607–1612.

[3] M. Saito, History of supercritical fluid chromatography: Instrumental development, J. Biosci. Bioeng. 115 (2013) 590–599.

[4] A. Grand-Guillaume Perrenoud, J.-L. Veuthey, D. Guillarme, Comparison of ultra-high performance supercritical fluid chromatography and ultra-high performance liquid chromatography for the analysis of pharmaceutical compounds, J. Chromatogr. A. 1266 (2012) 158–167.

[5] L. Sciascera, O. Ismail, A. Ciogli, D. Kotoni, A. Cavazzini, L. Botta, et al., Expanding the potential of chiral chromatography for high-throughput screening of large compound libraries by means of sub–2 µm Whelk-O 1 stationary phase in supercritical fluid conditions, J. Chromatogr. A. 1383 (2015) 160–168.
[6] F. Kamarei, F. Gritti, G. Guiochon, Investigation of the axial heterogeneity of the retention factor of carbamazepine along an supercritical fluid chromatography column. I – Linear conditions, J. Chromatogr. A. 1306 (2013) 89 – 96.
[7] M. Enmark, P. Forssén, J. Samuelsson, T. Fornstedt, Determination of adsorption isotherms in supercritical fluid chromatography, J. Chromatogr. A. 1312 (2013) 124–133.
[8] M. Enmark, J. Samuelsson, E. Forss, P. Forssén, T. Fornstedt, Investigation of plateau methods for adsorption isotherm determination in supercritical fluid chromatography, J. Chromatogr. A. 1354 (2014) 129–138.
[9] M. Enmark, D. Åsberg, J. Samuelsson, T. Fornstedt, The Effect of Temperature, Pressure and Co-Solvent on a Chiral Supercritical Fluid Chromatography Separation, Chrom. Today. 7 (2014) 14–17.
[10] D. Åsberg, M. Enmark, J. Samuelsson, T. Fornstedt, Evaluation of co-solvent fraction, pressure and temperature effects in analytical and preparative supercritical fluid chromatography, J. Chromatogr. A. 1374 (2014) 254 – 260.
[11] D. Yun, G. Li, A. Rajendran, Peak distortions arising from large-volume injections in supercritical fluid chromatography, Journal of Chromatography A. 1392 (2015) 91–99.
[12] J. Fairchild, J. Hill, P. Iraneta, Influence of Sample Solvent Composition for SFC Separations, LC GC N. AM. 31:4 (2013) 326–333.
[13] J. Samuelsson, P. Forssén, T. Fornstedt, Sample conditions to avoid pH distortion in RP-LC, J. Sep. Science. 36 (2013) 3769–3775.
[14] S. Keunchkarian, M. Reta, L. Romero, C. Castells, Effect of sample solvent on the chromatographic peak shape of analytes eluted under reversed-phase liquid chromatogaphic conditions, J. Chromatogr. A. 1119 (2006) 20–28.
[15] B.J. VanMiddlesworth, J.G. Dorsey, Quantifying injection solvent effects in reversed-phase liquid chromatography, J. Chromatogr. A. 1236 (2012) 77–89.
[16] C. Rana, A. De Wit, M. Martin, M. Mishra, Combined influences of viscous fingering and solvent effect on the distribution of adsorbed solutes in porous media, RSC Adv. 4 (2014) 34369–34381.
[17] L. Miller, Preparative enantioseparations using supercritical fluid chromatography, J. Chromatogr. A. 1250 (2012) 250–255.
[18] L.. Miller, I.. Sebastian, Evaluation of injection conditions for preparative supercritical fluid chromatography, J. Chromatogr. A. 1250 (2012) 256–263.
[19] B.S. Broyles, R.A. Shalliker, D.E. Cherrak, G. Guiochon, Visualization of viscous fingering in chromatographic columns, J. Chromatogr. A. 822 (1998) 173–187.
[20] R.. Shalliker, B.. Broyles, G. Guiochon, Visualization of viscous fingering in high-performance liquid chromatographic columns: Influence of the header design, J. Chromatogr. A. 865 (1999) 73–82.
[21] H.J. Catchpoole, R.A. Shalliker, G.R. Dennis, G. Guiochon, Visualising the onset of viscous fingering in chromatography columns, J. Chromatogr. A. 1117 (2006) 137–145.

[22] R.A. Shalliker, H.J. Catchpoole, G.R. Dennis, G. Guiochon, Visualising viscous fingering in chromatography columns: High viscosity solute plug, J. Chromatogr. A. 1142 (2007) 48–55.
[23] E.J. Fernandez, T.T. Norton, W.C. Jung, J.G. Tsavalas, A Column Design for Reducing Viscous Fingering in Size Exclusion Chromatography, Biotechnol. Prog. 12 (1996) 480–487.
[24] E.J. Fernandez, C.A. Grotegut, G.W. Braun, K.J. Kirschner, J.R. Staudaher, M.L. Dickson, et al., The effects of permeability heterogeneity on miscible viscous fingering: A three-dimensional magnetic resonance imaging analysis, Phys. Fluids. 7 (1995) 468–477.
[25] R.A. Shalliker, B.S. Broyles, G. Guiochon, Physical evidence of two wall effects in liquid chromatography, J. Chromatogr. A. 888 (2000) 1–12.
[26] G. Rousseaux, M. Martin, A. De Wit, Viscous fingering in packed chromatographic columns: Non-linear dynamics, J. Chromatogr. A. 1218 (2011) 8353–8361.
[27] K. Kato, M. Kokubo, K. Ohashi, A. Sato, D. Kodama, Correlation of High Pressure Density Behaviors for Fluid Mixtures made of Carbon Dioxide with Solvent at 313.15 K, Open Thermodyn. J. 3 (2009) 1–6.
[28] Kunz, O, Klimeck, R, Wagner, W, Jaeschke, M, The GERG-2004 Wide-Range Equation of State for Natural Gases and Other Mixtures., Fortschr.-Ber. VDI, VDI-Verlag, Düsseldorf, 2007.
[29] I.H. Bell, J. Wronski, S. Quoilin, V. Lemort, Pure and Pseudo-pure Fluid Thermophysical Property Evaluation and the Open-Source Thermophysical Property Library CoolProp, Ind. Eng. Chem. Res. 53 (2014) 2498–2508.
[30] G. Guiochon, D.G. Shirazi, A. Felinger, A.M. Katti, Fundamentals of preparative and nonlinear chromatography, 2nd ed., Academic Press, Boston, MA, 2006.
[31] I. Langmuir, The constitution and fundamental properties of solids and liquids. part i. solids, J. Am. Chem. Soc. 38 (1916) 2221–2295.
[32] P. Forssén, J. Lindholm, T. Fornstedt, Theoretical and experimental study of binary perturbation peaks with focus on peculiar retention behaviour and vanishing peaks in chiral liquid chromatography, J. Chromatogr. A. 991 (2003) 31–45.
[33] D. Tondeur, H. Kabir, L.A. Luo, J. Granger, Multicomponent adsorption equilibria from impulse response chromatography, Chem. Eng. Sci. 51 (1996) 3781–3799.
[34] J. Samuelsson, T. Fornstedt, Calculations of the energy distribution from perturbation peak data--A new tool for characterization of chromatographic phases, J. Chromatogr. A. 1203 (2008) 177–184.
[35] J. Samuelsson, R. Arnell, T. Fornstedt, Potential of adsorption isotherm measurements for closer elucidating of binding in chiral liquid chromatographic phase systems, J. Sep. Sci. 32 (2009) 1491–1506.
[36] J. Villadsen, M.L. Michelsen, Solution of Differential Equation Models by Polynomial Approximation, Prentice-Hall, Englewood Cliffs, NJ, 1978.
[37] K. Kaczmarski, M. Mazzotti, G. Storti, M. Mobidelli, Modeling fixed-bed adsorption columns through orthogonal collocations on moving finite elements, Comput. Chem. Eng. 21 (1997) 641–660.
[38] P.N. Brown, A.C. Hindmarsh, G.D. Byrne, Variable-Coefficient Ordinary Differential Equation Solver, available at: http://netlib.org.

[39] J. Samuelsson, T. Undin, A. Törncrona, T. Fornstedt, Improvement in the generation of adsorption isotherm data in the elution by characteristic points method--The ECP-slope approach, J. Chromatogr. A. 1217 (2010) 7215–7221.
[40] L.R. Snyder, Role of the solvent in liquid-solid chrornatography - a review, Anal. Chem. 46 (1974) 1384–1393.
[41] V. Abrahamsson, M. Sandahl, Impact of injection solvents on supercritical fluid chromatography, Journal of Chromatography A. 1306 (2013) 80–88.
[42] J.R. Strubinger, H. Song, J.F. Parcher, High-pressure phase distribution isotherms for supercritical fluid chromatographic systems. 2. Binary isotherms of carbon dioxide and methanol, Anal. Chem. 63 (1991) 104–108.
[43] P. Vajda, G. Guiochon, Modifier adsorption in supercritical fluid chromatography onto silica surface, J. Chromatogr. A. 1305 (2013) 293–299.
[44] K.S.W. Sing, Reporting physisorption data for gas/solid systems with special reference to the determination of surface area and porosity (Recommendations 1984), Pure Appl. Chem. 57 (1985).
[45] J. Samuelsson, P. Forssén, M. Stefansson, T. Fornstedt, Experimental Proof of a Chromatographic Paradox: - Are the Injected Molecules in the Peak?, Anal. Chem. 76 (2004) 953–958.
[46] J. Samuelsson, R. Arnell, J.S. Diesen, J. Tibbelin, A. Paptchikhine, T. Fornstedt, et al., Development of the Tracer-Pulse Method for Adsorption Studies of Analyte Mixtures in Liquid Chromatography Utilizing Mass Spectrometric Detection, Anal. Chem. 80 (2008) 2105–2112.
[47] J. Samuelsson, R. Arnell, T. Fornstedt, Invisible Analyte Peak Deformations in Single-Component Liquid Chromatography, Anal. Chem. 78 (2006) 2765–2771.
[48] J.L. Gohres, A.T. Marin, J. Lu, C.L. Liotta, C.A. Eckert, Spectroscopic Investigation of Alkylcarbonic Acid Formation and Dissociation in CO2-Expanded Alcohols, Ind. Eng. Chem. Res. 48 (2009) 1302–1306.
[49] P.R. Fields, T.L. Chester, A.M. Stalcup, Viscosity Estimation in Binary and Ternary Supercritical Fluid Mixtures Containing Carbon Dioxide Using a Supercritical Fluid Chromatograph, J. Liq. Chromatogr. Related Technol. 34 (2011) 995–1003.
[50] R.A. Shalliker, V. Wong, G. Guiochon, Reproducibility of the finger pattern in viscous fingering, J. Chromatogr. A. 1161 (2007) 121–131.

Figure Captions

Fig. 1: Schematic figure illustrating instrumental plumbing for (a) mixed stream injection and (b) modifier stream injection.

Fig. 2: Comparisons between mixed (black solid line) and modifier stream (grey solid line) injections of antipyrine and salicylanilide. In the top row 5, 30 and 75 µL injections of antipyrine. In (a) 0.25 g/L and in (b) 100 g/L. In the bottom row 5, 30 and 75 µL injections of salicylanilide. In (c) 0.5 g/L and in (b) 100 g/L.

Fig. 3: Observations of the peak distortion of antipyrine and salicylanilide when injected in SFC and NPLC mode. In (a) experiments conducted in SFC mode with 75 µL ca 0.2 g/L antipyrine injected in toluene (grey), ethanol (dashed grey) and methanol (black). Running conditions were 90/10 v% CO_2/MeOH. In (b) experiments conducted in NPLC mode with 75 µL of ca 0.2 g/L antipyrine injected in 2-propanol (grey), ethanol (dashed grey) and 85/15 v% heptane/EtOH. Running conditions 85/15 v% heptane/EtOH.

Fig. 4: Determined Langmuir adsorption isotherm parameters for antipyrine at different fractions of modifier are plotted. In (a) the monolayer saturation capacity and in (b) the association equilibrium constant is plotted. Symbols determined adsorption data and lines model fit to a cubic polynomial function.

Fig. 5: Experimental (a) and simulated (b, c) elution profiles of antipyrine is plotted. In (a) experimental elution profiles for 2, 5, 10, 20, 30, 60 and 75µL 0.25 g/L antipyrine in eluent containing 7.2 v% MeOH are plotted. In (b) corresponding simulated injections when the methanol plug is not retained and (c) same as in (b) but now the methanol is retained.

Fig. 6: Experimental (a,b) and simulated (c) MeOH elution profiles from 2, 30 and 60 µL injections. In (a) pure methanol is injected and recorded at 202 nm. In (b) deuterium labeled methanol (Mw=36 g/mol) is injected and detected using APCI-MS at 37 m/z. In (c) the calculated retained methanol elution profile described using the Langmuir model with q_s= 37 v%MeOH / L and K = 1.46 L/v%MeOH.

Fig. 7: Photographs illustrating the change in band-shape as a function of the viscosity contrast. In this experiments the refractive index system were matched with the stationary phase, so that the column becomes transparent. In both cases the viscosity of the injection plug was 0.38 cP. The injection volume was 5 µL, flow rate 0.5 mL/min. The column internal diameter was 5 mm, and the column length was 54 mm. Flow direction is from left to right. In (a) Mobile phase viscosity 0.38 cP, viscosity contrast around 0 and in (b) Mobile phase viscosity 1.44 cP, viscosity contrast about 3.8 times.

Table 1: Properties of solvents used this study [45].

Solvent	**Viscosity [cP]**	**$\varepsilon_0(SiO_2)$**	**Dielectric constant**
Heptane	0.42	0	1.92
Toluene	0.59	0.22	2.38
Isopropanol	2.40	0.60	20.33
Ethanol	1.10	0.68	24.55
Methanol	0.59	0.73	32.70

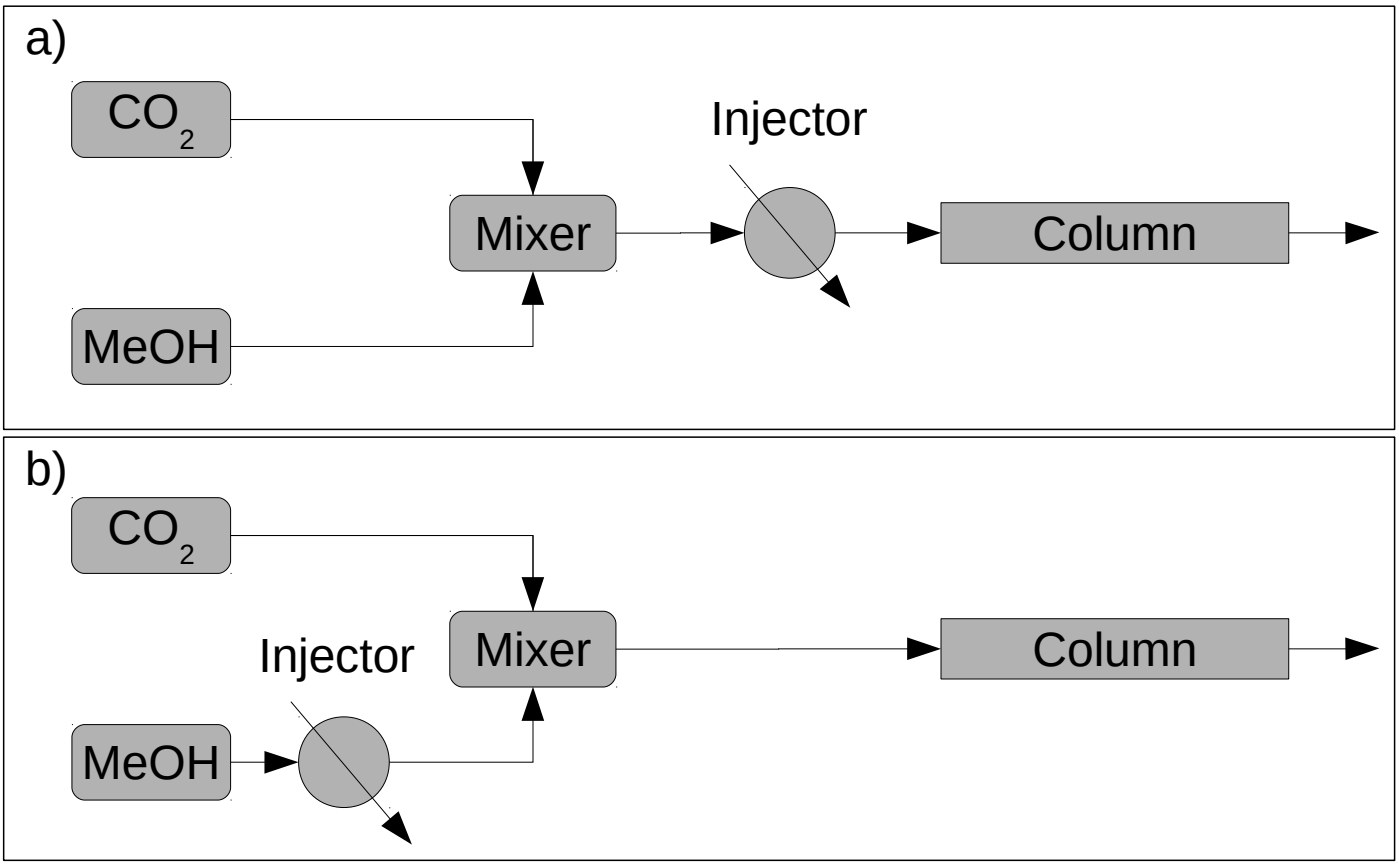
a)
CO2
MeOH
Mixer
Injector
Column
b)
CO2
MeOH
Injector
Mixer
Column

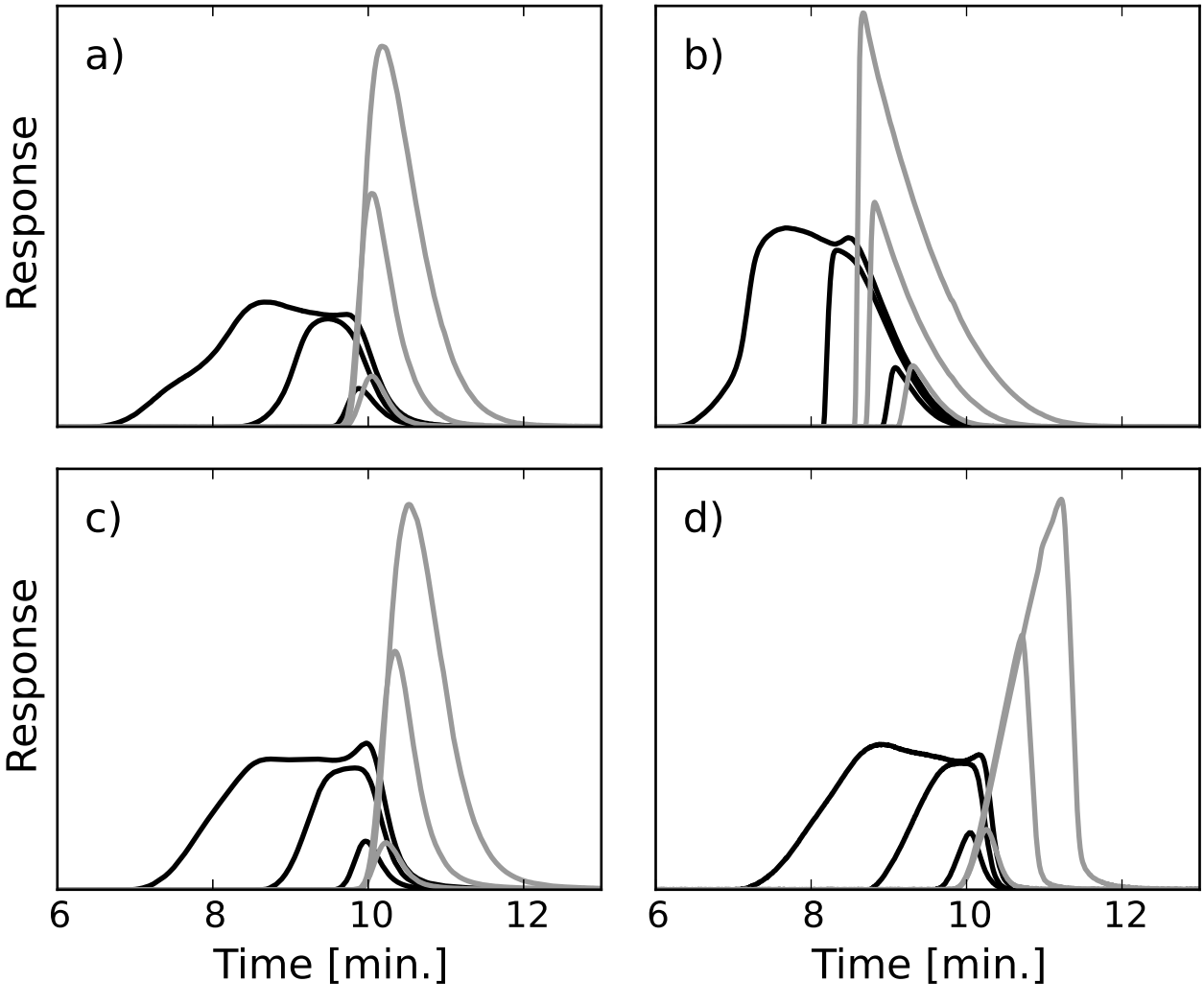
a)
b)
c)
d)
Response
Response
6
8
10
12
6
8
10
12
Time [min.]
Time [min.]

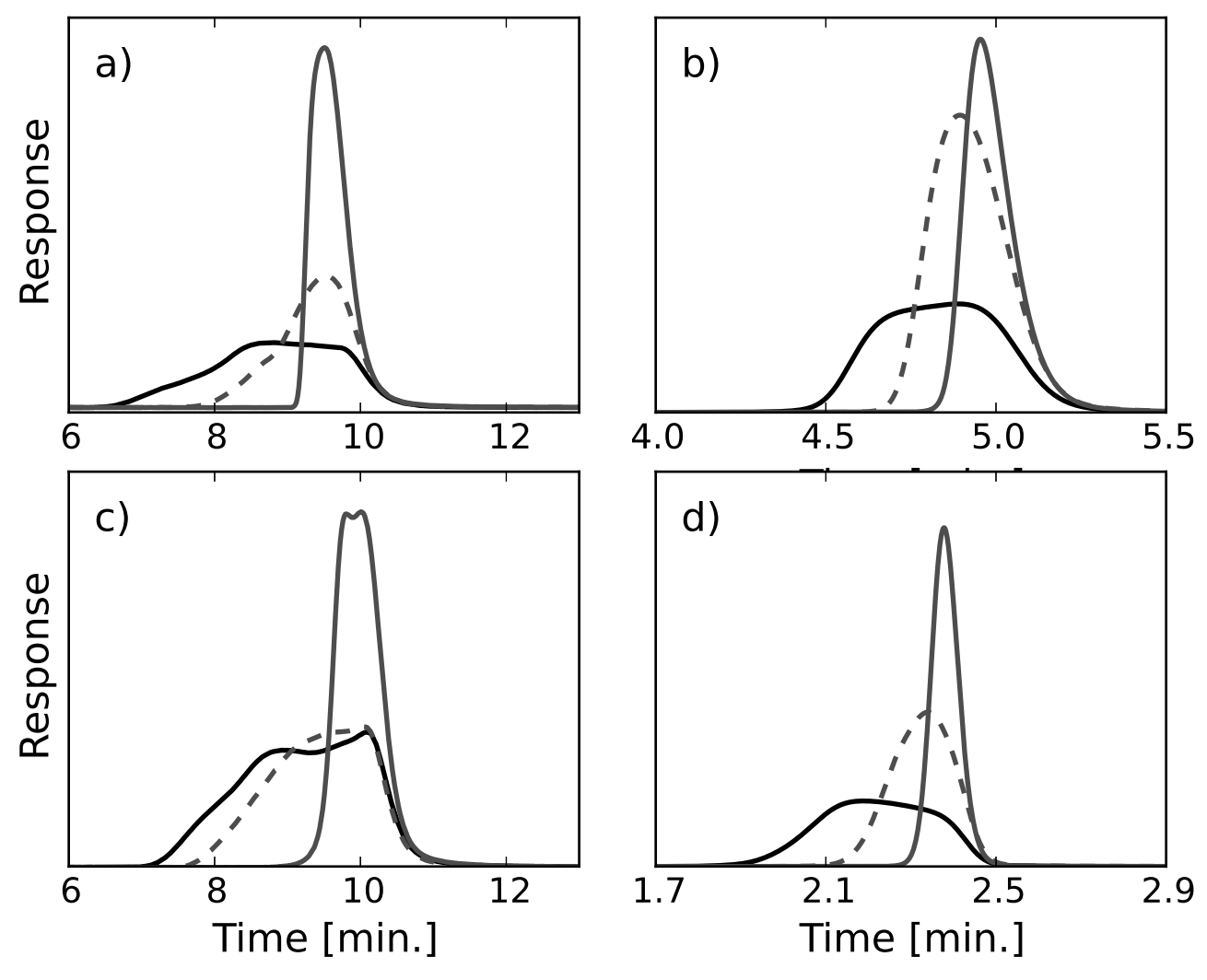
a)
b)
c)
d)
Response
Response
6
8
10
12
4.0
4.5
5.0
5.5
6
8
10
12
1.7
2.1
2.5
2.9
Time [min.]
Time [min.]

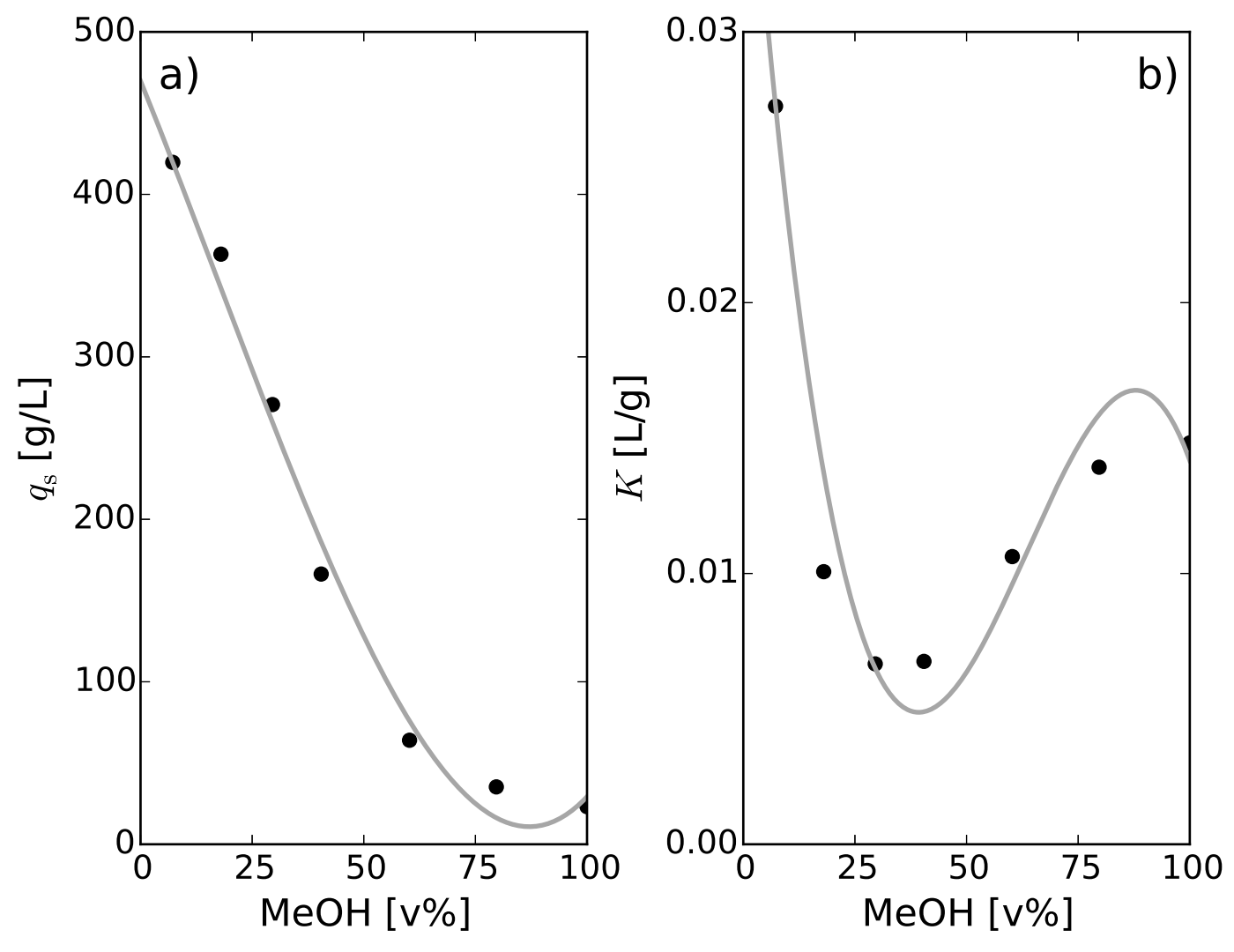
a)
b)
q_s [g/L]
K [L/g]
MeOH [v%]
MeOH [v%]
0
100
200
300
400
500
0.00
0.01
0.02
0.03
0
25
50
75
100

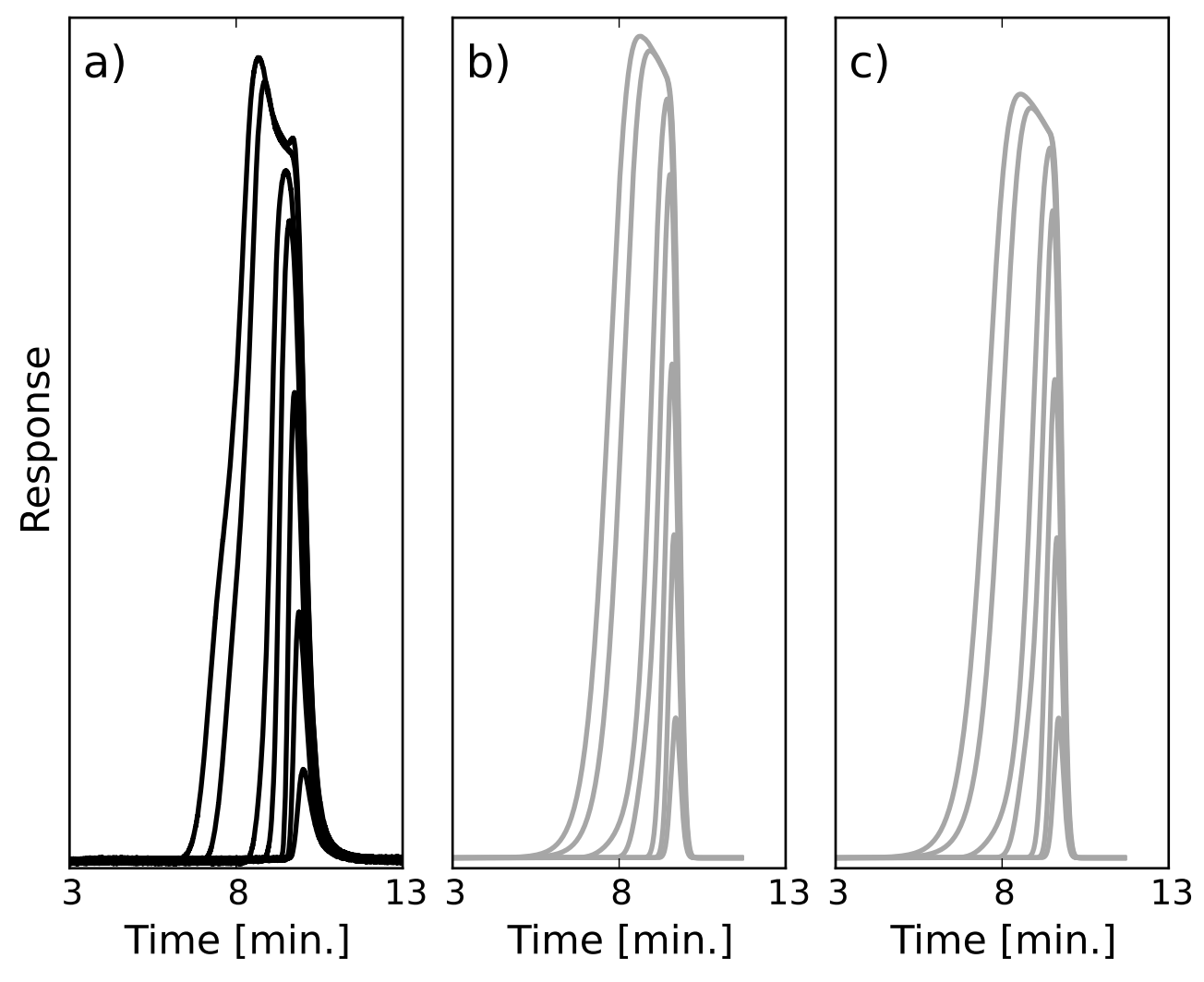
a)
b)
c)
Response
3
8
13
Time [min.]

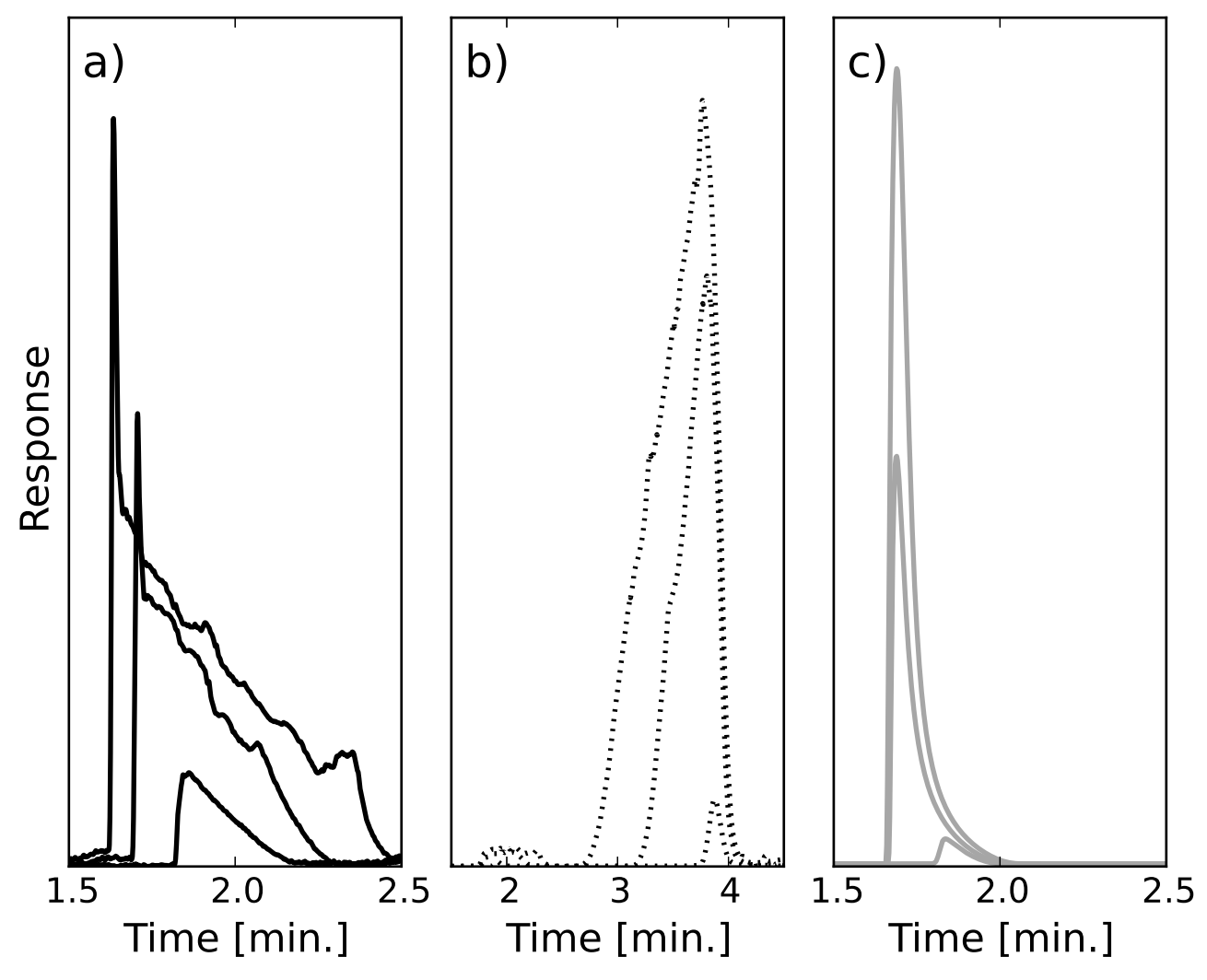
a)
b)
c)
Response
1.5
2.0
2.5
2
3
4
Time [min.]
Time [min.]
1.5
2.0
2.5
Time [min.]

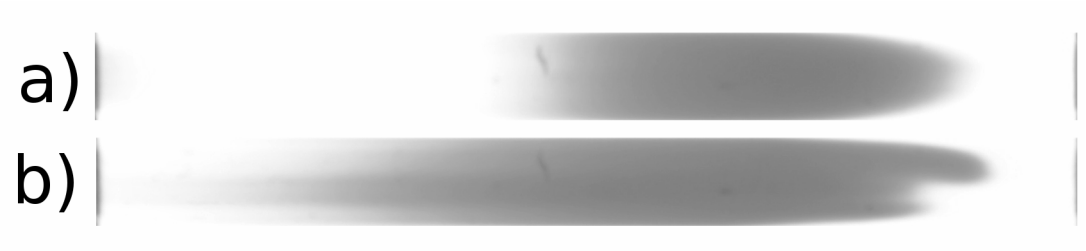
a)
b)


a)
b)